Fractal Analysis of Binding and Dissociation of Protein-Analyte Interactions on Biosensor Surfaces

Kennon Shelton and Ajit Sadana

Department of Chemical Engineering, University of Mississippi, P.O. Box 1848, University, MS 38677-1848, USA

A fractal analysis is presented for the binding and dissociation of two different protein-analyte interactions occurring on biosensor surfaces. The paper emphasizes the importance of the biosensor surface on the analyte-receptor interactions occurring on biosensor surfaces.

1. Introduction

The analysis of protein-anlayte interactions is an important and diversified area of application. Biosensors have often been employed to analyze these types of interactions. In this article we use fractal analysis to analyze (a) the binding and dissociation (if applicable) kinetics of (a) recombinant transthyretin (rTTR) in solution to T4 (*L*-thyroxine (T4) immobilized on a sensor chip surface using different spacers [[1], and (b) G_t (G protein transducin) in solution to different densities of Rho (rhodopsin) immobilized on a sensor chip surface [2].

2. Theory

Havlin [3] has reviewed and analyzed the diffusion of reactants towards fractal surfaces. The details of the theory and the equations involved for the binding and the dissociation phases for analyte-receptor binding are available [4]. The details are not repeated here; except that just the equations are given to permit an easier reading. These equations have been applied to other biosensor systems [4-6]. For most applications, a single- or a dual-fractal analysis is often adequate to describe the binding and the dissociation kinetics.

2.1 Single-fractal analysis

2.1.1 Binding rate coefficient.

Havlin [3] indicates that the diffusion of a particle (analyte [Ag]) from a homogeneous solution to a solid surface (e.g. receptor [Ab]-coated surface) on which it reacts to form a product (analyte-receptor complex; (Ab.Ag)) is given by:

$$(Ab \cdot Ag) \approx \begin{cases} t^{(3-D_{f,bind})/2} = t^{p} & t < t_c \\ t^{1/2} & t > t_c \end{cases} \quad (1)$$

Here $D_{f,bind}$ or D_f is the fractal dimension of the surface during the binding step. t_c is the cross-over value. Havlin [3] indicates that the cross-over value may be determined by $r_c^2 \sim t_c$. Above the characteristic length, r_c, the self-similarity of the surface is lost and the surface may be considered homogeneous. Above time, t_c the surface may be considered

homogeneous, since the self-similarity property disappears, and 'regular' diffusion is now present. For a homogeneous surface where D_f is equal to 2, and when only diffusional limitations are present, p = ½ as it should be.

2.1.2 Dissociation rate coefficient

The diffusion of the dissociated particle (receptor [Ab] or analyte [Ag]) from the solid surface (e.g., analyte[Ag]-receptor [Ab]) complex coated surface) into solution may be given, as a first approximation by:

$$(Ab.Ag) \approx -t^{(3-D_{f,diss})/2} = t^{p} \quad (t>t_{diss}) \tag{2}$$

Here $D_{f,diss}$ is the fractal dimension of the surface for the dissociation step. This corresponds to the highest concentration of the analyte-receptor complex on the surface. Henceforth, its concentration only decreases. The dissociation kinetics may be analyzed in a manner 'similar' to the binding kinetics.

2.2 *Dual-fractal analysis*

2.2.1 Binding rate coefficient

In this case, the product (antibody-antigen; or analyte-receptor complex, Ab.Ag or analyte.receptor) is given by:

$$(Ab.Ag) \approx \begin{cases} t^{(3-D_{f1,bind})/2} = t^{p1} & (t < t_1) \\ t^{(3-D_{f2,bind})/2} = t^{p2} & (t_1 < t < t_2) = t_c \\ t^{1/2} & (t > t_c) \end{cases} \tag{3}$$

In some cases, as mentioned above, a triple-fractal analysis with six parameters (k_1, k_2, k_3, D_{f1}, D_{f2}, and D_{f3}) may be required to adequately model the binding kinetics. This is when the binding curve exhibits convolutions and complexities in its shape due perhaps to the very dilute nature of the analyte or for some other reasons. Also, in some cases, a dual-fractal analysis may be required to describe the dissociation kinetics.

3. Results

At the outset it should be indicated that alternate expressions for fitting the binding and dissociation data are available that include saturation, first-order reaction, and no diffusional limitations, but these expressions are deficient in describing the heterogeneity that inherently exists on the surface. It is this heterogeneity on the biosensor surface that one is attempting here to relate to the different biosensor performance parameters. More specifically the question we wish to answer is that how may one change the heterogeneity or the fractal dimension, D_f on the biosensor chip surface in order that one may be able to enhance the different biosensor performance parameters.

Other modeling attempts also need to be mentioned. One might justifiably argue that appropriate modeling may be achieved by using a Langmuirian or other approach. The Langmuirian approach may be used to model the data presented if one assumes the presence of discrete classes of sites, for example double exponential analysis as compared with the single-fractal analysis. Lee and Lee [7] indicate that the fractal approach has been applied to surface science, for example, adsorption and reaction processes.

These authors emphasize that the fractal approach provides a convenient means to represent the different structures and morphology at the reaction surface. These authors also emphasize using the fractal approach to develop optimal structures and as a predictive approach. Another advantage of the fractal technique is that the analyte-receptor association is a complex reaction, and the fractal analysis via the fractal dimension and the rate coefficient provide a useful lumped parameter analysis of the diffusion-limited reaction occurring on a heterogeneous surface.

In a classical situation, to demonstrate fractality, one should make a log-log plot, and one should definitely have a large amount of data. It may be useful to compare the fit to some other forms, such as exponential, or involving saturation, etc. At present, we do not present any independent proof or physical evidence of fractals in the examples presented. Nevertheless, we still use fractals and the degree of heterogeneity on the biosensor surface to gain insights into enhancing the different biosensor performance parameters. The fractal approach is a convenient means (since it is a lumped parameter) to make the degree of heterogeneity that exists on the surface more quantitative. Thus, there is some arbitrariness in the fractal approach to be presented. The fractal approach provides additional information about interactions that may not be obtained by a conventional analysis of biosensor data. Here we are attempting to relate the fractal dimension, D_f or the degree of heterogeneity on the biosensor surface with the different biosensor performance parameters. More specifically, we are interested in finding out how changes in the fractal dimension or the degree of heterogeneity on the biosensor chip surface affect the different biosensor parameters of interest.

Unless specifically mentioned there is no nonselective adsorption of the analyte. In other words, nonspecific binding is ignored. Nonselective adsorption would skew the results obtained very significantly. In these types of systems, it is imperative to minimize this nonselective adsorption. We also do recognize that, in some cases, this nonselective adsorption may not be a significant component of the adsorbed material and that the rate of association, which is of a temporal nature would depend on surface availability.

Marchesini et al. [1] have recently developed a novel surface plasmon resonance-based biosensor to screen chemicals which exhibit thyroid-disrupting activity. These authors detected two thyroid transport proteins (TPs), thyroxine binding globulin (TBG) and recombinant transtyretin (rTTR) in solution using a CM5 sensor chip coated with *L*-thyroxine (T4) in a Biacore 3000 biosensor system. These authors indicate that *L*-thyroxine is the main hormone of the thyroid system. Lans et al. [8] and Hallgren and Darnerud [9] indicate that polyhalogenated aromatic hydrocarbons (PHAHs) and several hydroxylated metabolites interact with high affinity with transthyretin (rTTR).

Figure 1a shows the binding of 18.2 nM rTTR in solution to T4 immobilized on a CM5 sensor chip using the spacer E [1]. A single-fractal analysis is adequate to describe the binding and the dissociation kinetics. The values of the binding rate coefficient, k, the fractal dimension, D_f, the dissociation rate coefficient, k_d and the fractal dimension for the dissociation phase, D_{fd} are given in Table I. The values of the binding and the dissociation rate coefficient presented in Table Ia were obtained from a regression analysis using Corel Quattro Pro 8.0 (Corel Quattro Pro 8.0, 1997) to model the data using Eqs. (1a and b), wherein (Analyte.Receptor) = $kt^{(3 - D_f)/2}$ for a single-fractal analysis for the binding phase, and (Analyte-Receptor) = $kt^{(3 - D_{f1})/2}$ and $kt^{(3 - D_{f2})/2}$ for a dual-fractal analysis. The binding rate coefficient values presented in Table 1a are within 95% confidence values. For example, for the binding 18.2 nM rTTR in solution to T4 immobilized on the CM5 sensor chip using the spacer E the binding rate coefficient, k is equal to 10.289 ± 0.352. The 95 % confidence limit indicates that the k values lie between 9.937 and 10.641. This indicates that the values are precise and significant.

Figure 1b shows the binding of 18.2 nM rTTR in solution to T4 immobilized on a CM5 sensor chip using the spacer F. Once again, a single-fractal analysis is adequate to describe the binding and the dissociation kinetics. The values of the binding rate coefficient, k, the fractal dimension, D_f, the dissociation rate coefficient, k_d and the fractal dimension for the dissociation phase, D_{fd} are given in Table I.

Figure 1c shows the binding of 18.2 nM rTTR in solution to T4 immobilized on a CM5 sensor chip using the spacer D. Once again, a single-fractal analysis is adequate to describe the binding and the dissociation kinetics. The values of the binding rate coefficient, k, the fractal dimension, D_f, the

dissociation rate coefficient, k_d and the fractal dimension for the dissociation phase, D_{fd} are given in Table I.

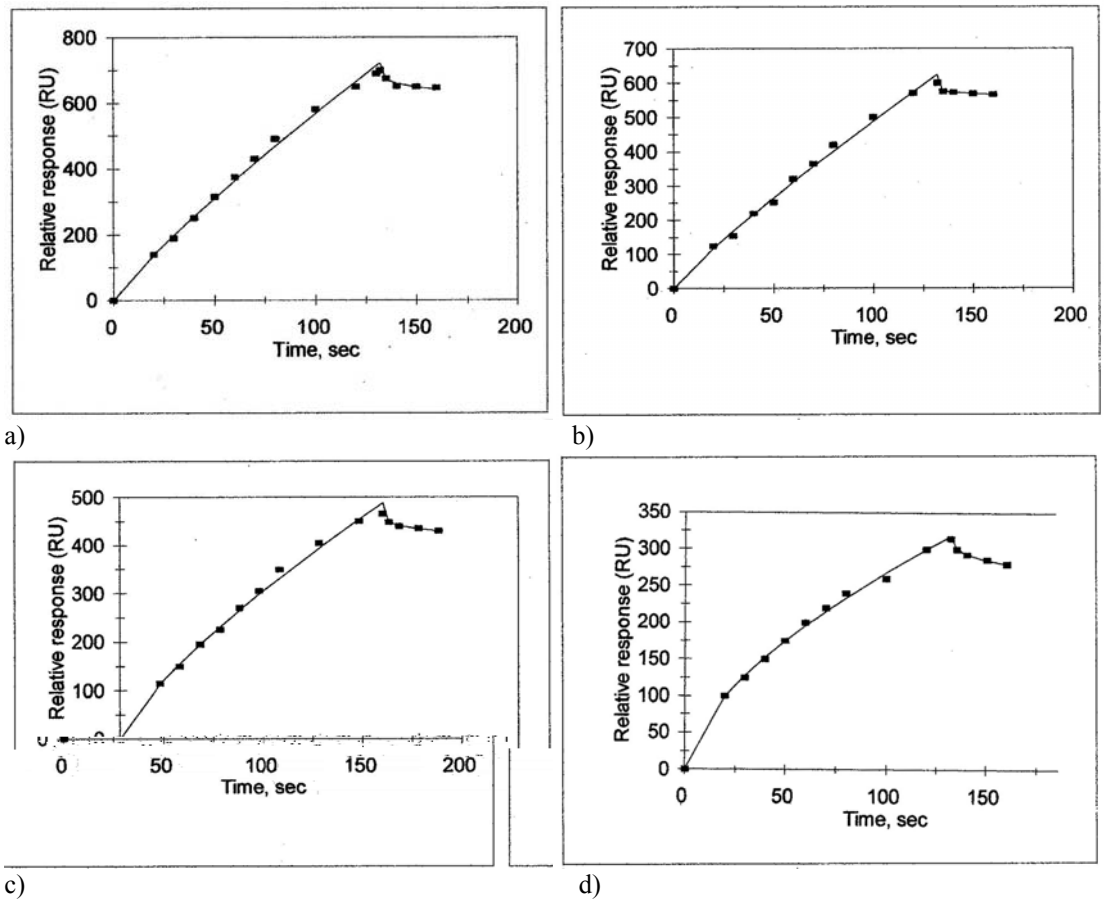

Figure 1:Binding and dissociation of 18.2 nM rTTR (recombinant transthyretin) in solution to T4 (*L*-thyroxine) immobilized on a sensor chip surface using different spacers [1]: (a) E (b) F (c) D (d) C

Figure 1d shows the binding of 18.2 nM rTTR in solution to T4 immobilized on a CM5 sensor chip using the spacer C. Once again, a single-fractal analysis is adequate to describe the binding and the dissociation kinetics. The values of the binding rate coefficient, k, the fractal dimension, D_f, the dissociation rate coefficient, k_d and the fractal dimension for the dissociation phase, D_{fd} are given in Table I.

Table I and Figure 2a show the increase in the binding rate coefficient, k with an increase in the fractal dimension, D_f. For the data shown in Figure 2a and in Table I, the binding rate coefficient, k is given by:

$$k = (6.652 \pm 0.598)\, D_f^{\,1.505 \pm 0.302} \qquad (2a)$$

The fit is good. Only four data points are available. The availability of more data points would lead to a more reliable fit. The binding rate coefficient, k is quite sensitive to the fractal dimension, D_f or the degree of heterogeneity that exists on the surface as noted by the close to one and one-half (equal to 1.505) order of dependence exhibited.

Table I and Figure 2b show the increase in the affinity (k/k_d) with an increase in the ratio of the fractal

dimensions (D_f/D_{fd}). For the data shown in Figure 2b and in Table I, the affinity (k/k_d) is given by:

$$k/k_d = (2.633 \pm 1.679)\,(D_f/D_{fd})^{2.945 \pm 1.821} \qquad (2b)$$

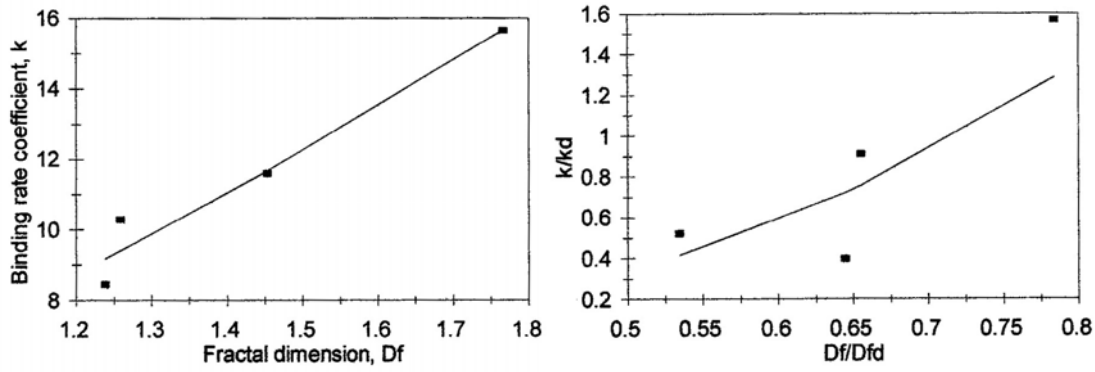

Figure 2: (a) Increase in the binding rate coefficient, k with an increase in the fractal dimension, D_f
(b) Increase in the affinity ($=k/k_d$) with an increase in the fractal dimension ratio, D_f/D_{fd}

Table I Binding and dissociation rate coefficients and fractal dimensions for the binding and the dissociation phases for 18.2 nM rTTR (recombinant transthyretin) in solution to T4 (*L*-thyroxine) immobilized on a CM5 sensor chip with different spacers (E. F, D and C) [1]

Spacer	k	k_d	D_f	D_{fd}
E	10.289 ± 0.352	19.760 ± 4.033	1.2586 ± 0.0342	2.3538 ± 0.2182
F	8.4600 ± 0.4197	21.399 ± 0.409	1.7614 ± 0.0529	2.7324 ± 0.0222
D	11.212 ± 0.378	12.334 ± 0.549	1.5466 ± 0.0362	2.3704 ± 0.0512
C	15.646 ± 0.328	9.977 ± 0.150	1.766 ± 0.0226	2.2516 ± 0.0176

The fit is good. Only four data points are available. The availability of more data points would lead to a more reliable fit. The affinity (k/k_d) is sensitive to the ratio of the fractal dimensions, (D_f/D_{fd}) as noted by the close to third (equal to 2.945) order of dependence exhibited.

Komolov et al. [2] have used SPR (surface plasmon resonance) spectroscopy to analyze protein-protein interactions in real time. These authors developed a simple biosensor-based approach to monitor the interactions between G protein transducin (G_t) and rhodopsin (Rho). Rhodopsin is a G protein-coupled receptor (GPCR). These authors indicate that GPCRs serve key functions in hormone, neurotransmitter, and sensory signaling. They do indicate that evanescent wave-based biosensor systems have been used previously to analyze G_t-Rho interactions [11-14]. However, the results obtained were heterogeneous. Komolov et al. [2] indicate that they have developed a robust biosensor system to analyze G_t-Rho interactions.

Figure 3a shows the binding of 0.7 μM G_t in solution to 8.05 x 10^{10} Rho/mm^2 (density) immobilized on a sensor chip surface. These authors wanted to analyze the influence of different densities of Rho immobilized on the sensor surface on the binding of G_t. A dual-fractal analysis is required to adequately describe the binding kinetics. The values of (a) the binding rate coefficient, k and the fractal dimension, D_f for a single-fractal analysis, (b) the binding rate coefficients, k_1 and k_2 , and the fractal dimensions, D_{f1} and D_{f2} for a dual-fractal analysis are given in Table II.

It is of interest to note that for a dual-fractal analysis, as the fractal dimension increases by a factor of 1.85 from a value of D_{f1}equal to 1.2082 to D_{f2} equal to 2.2388, the binding rate coefficient value increases by a factor of 14.0 from a value of k_1 equal to 7.445 to k_2 equal to 104.298. Note that changes

in the degree of heterogeneity on the biosensor surface (or the fractal dimension value) and in the binding rate coefficient are in the same direction.

Figure 3b shows the binding of 0.7 μM G_t in solution to 2.98 x 10^{10} Rho/mm^2 (density) immobilized on a sensor chip surface. Once again, a dual-fractal analysis is required to adequately describe the binding kinetics. The values of (a) the binding rate coefficient, k and the fractal dimension, D_f for a single-fractal analysis, and (b) the binding rate coefficients, k_1 and k_2 , and the fractal dimensions, D_{f1} and D_{f2} for a dual-fractal analysis are given in Table II.

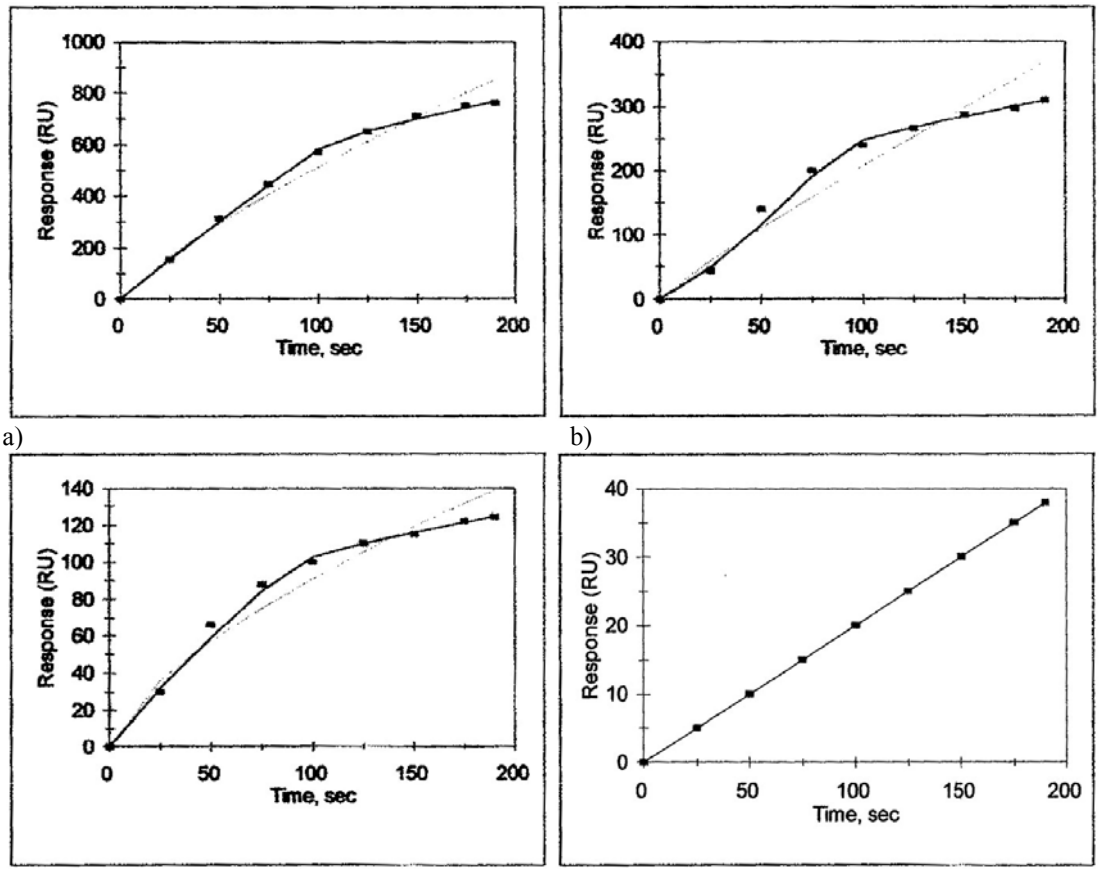

Figure 3: Binding of G_t (G protein transducin) in solution to different densities of Rho (rhodopsin) immobilized on a sensor chip [2]:

(a) 8.05 x 10^{10} Rho/mm^2
(b) 2.98 x 10^{10} Rho/mm^2
(c) 1.4 x 10^{10} Rho/mm^2
(d) 0.54 x 10^{10} Rho/mm^2

Once again for a dual-fractal analysis, as the fractal dimension increases by a factor of 4.466 from a value of D_{f1} equal to 0.5152 to D_{f2} equal to 2.301, the binding rate coefficient value increases by a factor of 55.15 from a value of k_1 equal to 0.8957 to k_2 equal to 49.399. Note that changes in the degree of heterogeneity on the biosensor surface (or the fractal dimension value) and in the binding rate coefficient are, once again, in the same direction.

Figure 3c shows the binding of 0.7 μM G_t in solution to 1.4 x 10^{10} Rho/mm^2 (density) immobilized on a sensor chip surface. Once again, a dual-fractal analysis is required to adequately describe the binding kinetics. The values of (a) the binding rate coefficient, k and the fractal dimension, D_f for a single-fractal

analysis, and (b) the binding rate coefficients, k_1 and k_2 , and the fractal dimensions, D_{f1} and D_{f2} for a dual-fractal analysis are given in Table II.

Figure 3d shows the binding of 0.7 μM G_t in solution to 0.54 x 10^{10} Rho/mm^2 (density) immobilized on a sensor chip surface. Once again, a dual-fractal analysis is required to adequately describe the binding kinetics. The values of (a) the binding rate coefficient, k and the fractal dimension, D_f for a single-fractal analysis, and (b) the binding rate coefficients, k_1 and k_2, and the fractal dimensions, D_{f1} and D_{f2} for a dual-fractal analysis are given in Table II.

Figure 4a and Table II show the increase in the binding rate coefficient, k_1 with an increase in the rhodopsin density (in Rho/mm^2) on the sensor chip surface. For the data shown in Figure 4a, the binding rate coefficient, k_2 is given by:

$$k_1 = (0.841 +/- 1.595) \text{ [density of rhodopsin, Rho/mm}^2\text{]}^{\,0.849 \pm 0.830} \qquad (3a)$$

There is scatter in the data. This is reflected in the error in the binding rate coefficient. Only the positive value is presented, since the binding rate coefficient cannot have a negative value. Only three data points are available. The availability of more data points would lead to a more reliable fit. The binding rate coefficient, k_1 exhibits less than a first (equal to 0.849) order of dependence on the density of rhodopsin (in Rho/mm^2) on the sensor chip surface.

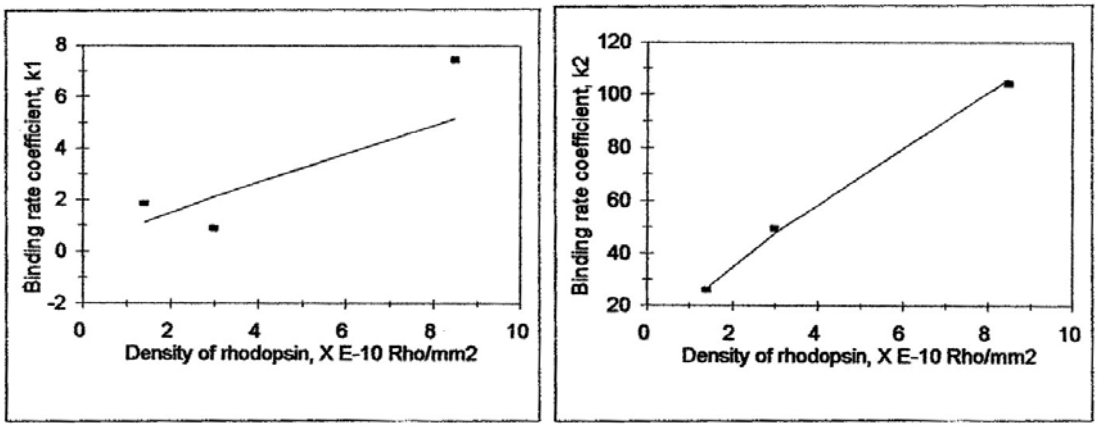

a) b)

Figure 4: (a) Increase in the binding rate coefficient, k_1 with an increase in the rhodopsin density
(b) Increase in the binding rate coefficient, k_2 with an increase in the rhodopsin density

Table II Binding rate coefficients and fractal dimensions for the binding of 0.7 μM G_t (G protein transducin) in solution to different densities of Rho (rhodposin, a prototypical G protein-coupled receptor (GPCR)) immobilized on a sensor chip surface [2].

Rhodopsin density	k	k_1	k_2	D_f	D_{f1}	D_{f2}
8.05 x 10^{10} Rho/mm^2	13.445 ± 1.313	7.445 ± 0.199	104.298 ± 1.396	1.4178 ± 0.101	1.2082 ± 0.0508	2.2388 ± 0.0832
2.98 x 10^{10} Rho/mm^2	3.287 ± 0.777	0.8957 ± 0.1795	49.399 ± 0.525	1.200 ± 0.231	0.5152 ± 0.0351	2.301 ± 0.0662
1.4 x 10^{10} Rho/mm^2	4.297 ± 0.628	1.8504 ± 0.2215	26.106 ± 0.184	1.6734 ± 0.148	1.2294 ± 0.2172	2.4054 ± 0.0442
0.54 x 10^{10} Rho/mm^2	0.2 ± 0	na	na	2.0 ± 1.3E-14	na	na

Figure 4b and Table II show the increase in the binding rate coefficient, k_2 with an increase in the rhodopsin density (in Rho/mm^2) on the sensor chip surface. For the data shown in Figure 4b, the binding rate coefficient, k_2 is given by:

$$k_2 = (20.636 +/- 0.99) [\text{density of rhodopsin, Rho/mm}^2]^{\,0.765 \pm 0.0366} \qquad (3b)$$

The fit is good. Only three data points are available. The availability of more data points would lead to a more reliable fit. The binding rate coefficient, k_2 exhibits less than a first (equal to 0.756) order of dependence on the density of rhodopsin (in Rho/mm^2) on the sensor chip surface. Note that the binding rate coefficient, k_1 exhibits a slightly higher order of dependence than k_2 on the rhodopsin density on the sensor chip surface.

4. Conclusion

A fractal analysis is presented for the binding and dissociation (where ever applicable) of protein-analyte interactions occurring on biosensor surfaces. Both, a single- and a dual-fractal analysis is used to model the binding and the dissociation kinetics. The binding and dissociation (where ever applicable) is presented for (a) rTTR in solution to T4 immobilized on a CM5 sensor chp surface using different spacers [1], and the interactions of G protein transducin (G_t) in solution to rhodopsin (Rho) immobilized on a sensor chip surface [2]. The fractal analysis emphasizes the importance of the biosensor surface on the interactions occurring on the surface, and helps provide physical insights into these interactions.

References

[1] Marchesini GR, E. Muelenberg, W. Haasnoot, M. Miziguchi, and H. Irth (2006). Biosensor recognition of thyroid-disrupting chemicals using transport proteins. Analytical Chemistry, 78, 1107-1114.
[2] Komolov KE. II Senin, PP Phillippov, and KW Koch (2006). Surface plasmon resonance study of G-Protein receptor coupling in a lipid bilayer-free system. Analytical Chemistry, 78, 1228-1234.
[3] Havlin S, Molecular diffusion and reaction, in *The Fractal Approach to Heterogeneous Chemistry: Surfaces, Colloids, Polymers*, (ed, D. Avnir), Wiley, New York, 1989, pp. 251-269.
[4] Sadana A (2001). A fractal analysis for the evaluation of hybridization kinetics in biosensors. *Journal of Colloid and Interface Science*, 151(1), 166-177.
[5] Sadana A (2005) Fractal Binding and Dissociation Kinetics for Different Biosensor Applications, Elsevier, Amsterdam.
[6] Ramakrishnan A, and A Sadana (2001). A single-fractal analysis of cellular analyte-receptor binding kinetics using biosensors. Biosystems, 59, 35-51.
[7] Lee CK, and SL Lee (1995). Multi-fractal scaling analysis of reactions over fractal surfaces. Surface Science, 325. 294-310.
[8] Lans MC, E Klasson-Wehler, M Willemsen, E Meussen, S Safe, and A Brouwer (1993). *Chemical and Biological Interactions*, 88, 7-21.
[9] Halgren S and PO Darnerud (2002). *Toxicology*, 177, 227-243.
[10] Corel Quattro Pro 8.0, Corel Corporation, Ottawa, Canada, 1997
[11] Bieri C, O Ernst, S Heyse, KP Hoffmann, and H Vogel (1999) *Nature Biotechnolog,* 17, 1105-1108.
[12] Minic J, J Grosclaude, J Aioun, MA Persuy, T Gorojankina, R Salesse, E Pajot-Augy, Y Hou, S Helali, N Jaffrezic-Renault, F Bessueille, A Errachid, G Gomila, O Ruiz, and J Samitier (2005). Biochimica Biophysica Acta, 1724, 324-332.
[13] Karlsson OP, and S Lofas, (2002). *Analytical Biochemistry*, 300, 1332-1338.